

Comparison of hydration water properties of common and durum wheat brans upon grinding with different loading modes

Reine Barbar^{a,*}, Claire Mayer-Laigle^a, Johnny Beaugrand^b, Bernard Cuq^a, Cécile Barron^a

^a IATE, Univ Montpellier, INRAE, Institut Agro Montpellier, France

^b INRAE, UR BIA, Nantes, France

ARTICLE INFO

Keywords:

Mechanical loading mode
Grinding
Water mobility
Bran structure

ABSTRACT

Wheat bran brings healthy properties in food products. However, its incorporation requires a first milling step during which it is subject to various loading modes which have an influence on its properties. This study investigated the influence of the loading modes (high shear or impact) generated by grinders during the milling on the hydration properties of common and durum wheat brans. An original study at molecular scale to target the distribution and intensity of hydration water bonds was carried out by gravimetric and spectroscopic methods. Results were analyzed in regards to the particle size distribution and shape factors as well as biochemical composition to highlight the process-structure-function relationships at macro and microscales. Impact grinder has a stronger effect on water vapor sorption capacity and FTIR multimer water at 3600 cm^{-1} of durum wheat bran as well as a red shift in the band at 1030 cm^{-1} related to a high decrease in residual starch crystallinity degree (about 17%). High shear grinder tends to increase the proportion of water strongly bound. Low field NMR analysis revealed differences in the high mobility water peak and a significant lower relaxation time T2 for native and ground durum wheat bran (up to 1.7 fold less).

1. Introduction

Wheat bran is a by-product of conventional wheat milling which is currently undervalued as only 10% is currently used for food applications (Onipe et al., 2015). It has been demonstrated that bran consumption has a positive effect on health by decreasing the risk of cardiovascular diseases (Wu et al., 2015), increasing fecal bulk and reducing intestinal transit time (Stevenson et al., 2012).

To incorporate bran into food product, wheat bran is often reduced into a fine powder (Onipe et al., 2015) involving a milling step. This step has to face the difficulty of wheat bran being a multilayered material made-up of different tissues including the outer pericarp, the inner pericarp, the hyaline band and testa, the aleurone layer and residual starchy endosperm. These different tissues have distinct compositions, nutritional, functional and contrasting mechanical properties (Ciccoritti et al., 2017). During the milling, the bran is subjected to mechanical stresses generated by the grinder such as compression, impact, friction, shear and extension, (Mayer-Laigle et al., 2018) that can influence its functional properties and so the quality of the final food products

(Deroover et al., 2020). A better understanding of the influence of the milling step on hydration properties could bring new insight for a better processing of healthy food products. It is the aim of the present study in which the effect of different mechanical loading modes on the hydration water properties of common and durum wheat brans during milling are compared.

Hydration properties are often assessed in a functional way by swelling, water retention, water absorption and porosity. These methods are quick but do not allow to evaluate the binding strengths between water and the bran matrix. In this study, we describe hydration properties of ground brans by functional and molecular approaches. This analysis is carried out in close relation to mechanical loading of the grinders and the intrinsic properties of each type of bran.

2. Materials and methods

2.1. Raw materials

The wheat bran was produced by a French industrial miller from

Abbreviations: ATR-FTIR, Attenuated Total Reflectance-Fourier Transform Infrared spectroscopy; NMR, Nuclear Magnetic Resonance; BET, Brunauer-Emmett-Teller; GAB, Guggenheim, Anderson and de Boer; SEM, Scanning electron microscopy; FID, Free induced decay.

* Corresponding author.

E-mail address: reine.barbar@supagro.fr (R. Barbar).

<https://doi.org/10.1016/j.jcs.2023.103786>

Received 20 October 2022; Received in revised form 10 July 2023; Accepted 15 September 2023

Available online 22 September 2023

0733-5210/© 2023 Elsevier Ltd. All rights reserved.

Fructidor variety, harvest in 2019. The durum wheat bran was produced by a French industrial miller (Panzani group) from a mixture of different durum wheat grain varieties (Miradou, Anvergur, Voilur, Claudio) without prior dehulling.

2.2. Grinding operations

The two native brans were ground using two grinding technologies in two different configurations:

An impact mill (Hosokawa-Alpine, type 100 UPZ, Augsburg, Germany), with a selection grid of 500 or 300 μm operating at a speed of 18 000 rpm. Milling was carried out at ambient temperature. In these configurations impact is the predominant loading mode.

An ultra-centrifugal mill ZM 200 (Retsch, Germany), a high speed rotor mill operated at a speed of 18 000 min^{-1} , with a selection grid of 500 or 250 μm . In this device shear is the predominant loading mode but impact is also present to a lesser extent. Prior to the milling raw bran was frozen and during the grinding a cyclone was used in order to additionally cool the sample by the air stream.

2.3. Bran characterization

2.3.1. Particle size measurement by laser diffraction

The particle size distribution of the ground samples was measured by laser diffraction using a Mastersizer 2000 equipped with a Scirocco 2000 dry dispersion unit Scirocco 2000 (Malvern Instruments, Worcestershire, UK). The particle size distribution is expressed as % of total particle volume. The median particle size (D_{50}) and span ($D_{90}-D_{10}/D_{50}$) were used as the primary descriptors. This measurement was performed only on ground material since the size of initial brans was outside the measurement range of the device. All measurements were performed in triplicate.

2.3.2. Morphological characteristics of starting material

Morphologi 4 (Malvern, United Kingdom) provides detailed morphological descriptions of particulate samples through static image analysis. Native bran particles were either manually dispersed (common wheat bran) or automatically with a sample dispersion unit (durum wheat bran) on a glass plate. Results are expressed by combining data over 5 plates to have a greater representativeness of the sample (with a total number of about 71 000 and 330 000 particles for common and durum wheat bran, respectively). Optic with a magnification of 2.5 was selected. The device captures a two dimensional image of the particles and circle equivalent diameter (diameter of a circle which has the same area as the particle) and high sensitivity circularity (HS: ratio of the particle's projected area to the particle's perimeter squared (eq. (1)) were calculated from the image. HS circularity expresses the surface roughness of the particle. A value of 1 corresponds to a perfectly smooth spherical particle

$$\text{HS circularity} = 4\pi \text{Area} / \text{Perimeter}^2 \quad (1)$$

The distributions were expressed in volume. Some samples were also analyzed using an SEM (Model Phenom, Thermo Fisher Scientific, US) with an accelerating voltage (10 kV).

2.3.3. Content in dry matter, ash, starch and damaged starch

The dry matter and ash contents of the native brans and ground fractions were determined according to approved AACC methods 44–19 and 08–12 respectively. Total starch content of fractions was measured in duplicate using Megazyme kit (Megazyme International Ireland Ltd., Ireland) according to approved AACC method 76–13. Damaged starch

was also determined on initial and ground fractions with a Megazyme kit (K-SDAM starch damage assay kit, Megazyme Int., Ireland) according to method AACCI N76–31.01.

2.3.4. Monosaccharides content

The polysaccharides were depolymerized before monosaccharides being quantified individually. The protocol from Barteau et al. (2021) was followed using inositol as an internal standard. After an acidic hydrolysis step, neutral monosaccharides were analyzed as their alditol acetate derivatives by gas chromatography-flame ionization detection (GC-FID). Standards of carbohydrate solutions were used for calibration. Analyses were performed in three independent assays. The total monosaccharide content is the sum of each monosaccharide amount and is expressed as the percentage of the dry matter mass.

2.3.5. Uronic acids content

Quantification of uronic acids was performed after wheat bran acid hydrolysis according to Beaugrand et al. (2004a). Uronic acid in acid hydrolysates were then quantified using the methoxydiphenyl colorimetric method (Blumenkr and Asboehan, 1973). All tests were done in triplicate.

2.3.6. Lignin content

The lignin content was determined from the powdered samples by the Klason method. For this gravimetric method, the lignin as the acid insoluble residue was determined using the non-hydrolyzable acid residue remaining after sulfuric acid hydrolysis (Monties, 1984).

2.3.7. Water vapor adsorption isotherms

Bran samples were dried to constant weight over phosphorus pentoxide in a vacuum climatic chamber at 40 °C, then placed over saturated salt solutions (NaCl, K_2SO_4 , KCl, KOH, NaBr, K_2CO_3) in desiccators at constant temperature (25 °C) to provide different water activities (0.08, 0.43, 0.57, 0.75, 0.85, and 0.97, respectively). Final water contents were determined when moisture equilibrium had been obtained. The water content of the samples was plotted against relative humidity for the two different native and ground brans. Experiments were conducted in duplicate. Guggenheim, Anderson and de Boer (GAB) equation was used to model water sorption curves (eq. (2)):

$$W = \frac{(m_0 C k a_w)}{(1 - k a_w)(1 - k a_w + C k a_w)} \quad (2)$$

Where W (g water/g dry matter) is the water content of the sample; a_w is the water activity; m_0 (g water/g dry matter) is the water content corresponding to the saturation of all primary adsorption sites by one water molecule; C is the Guggenheim constant. k is the factor correcting properties of the multilayer molecules with respect to the bulk liquid. The experimental data were fit with the software Microsoft Excel 2016 by using the method of the least squares methods.

The solid surface area (A) of samples can be calculated from the monolayer water content (M_0) according to eq. (3) (Mazza and Le Maguer, 1978):

$$A = M_0 \left(\frac{1}{M_{H_2O}} \right) (N) (A_{H_2O}) = (3.5 \times 10^6) M_0 \quad (3)$$

Where A is the solid surface area (m^2/kg solid); M_{H_2O} is the molecular weight of water molecule (18 kg/kmol); N is the Avogadro's number (6×10^{26} molecules/kmole); A_{H_2O} is the area of a water molecule (10.6 Å). Modeling of the experimental data using the GAB model was carried out on the mean values of the 2 series of measurements. The quality of the fit

of the model was assessed by calculating the RMSE and R2 values. The value of the root-mean-square error (RMSE) was calculated as follows:

$$RMSE = \sqrt{\frac{\sum [W_i - W_{i*}]^2}{N}} \quad (4)$$

with N: the number of experimental points; W_i : the average experimental water content; W_{i*} : the calculated water content.

2.3.8. ATR-FTIR spectra

The FTIR spectra were collected in the 400–4000 cm^{-1} wavenumber range on a Bruker Vertex 70v Fourier Transform spectrometer (Bruker Optik GmbH, Germany) operating with a Globar source in combination with a KBr beamsplitter and a DigiTect DLATGS detector with integrated preamplifier. The optical cell was a Golden Gate diamond ATR system. The spectra were recorded with a resolution of 4 cm^{-1} , automatically adding 128 repetitive scans. Scans were corrected for the air contribution and were preprocessed using OPUS software (version 7.0) by performing a baseline correction, a 9 points smoothing and a vector normalization for taking into account the effective number of absorbers. Experiments were conducted on powders of native and ground brans previously equilibrated at 40 or 58% relative humidities in specific climatic chambers (at 25 °C). The spectra of freeze dried brans were subtracted following the direct difference method (Poole and Finney, 1982). The resulting spectrum is supposed to correspond to interfacial hydration water.

ATR-FTIR spectra were also analyzed to determine the crystallinity of starch granules. The bands in the region 1100–900 cm^{-1} have been shown to be sensitive to changes in starch structure, in particular bands at 1000, 1022 and 1047 cm^{-1} . The band around 1022 cm^{-1} seems to increase in more amorphous samples, while the bands around 1000 and 1047 cm^{-1} become more defined in more crystalline samples.

2.3.9. Low field NMR measurements

Transversal relaxation times (T_2) were obtained from time domain nuclear magnetic resonance (TD-NMR) measurements using a Minispec mq spectrometer (minispec mq20, Bruker, France) operating at a frequency of 20 MHz (0.47 T). A Free Induced Decay (FID) Carrel-Purcell-Meiboom-Gill (CPMG) sequence with an acquisition time of 0.15 ms and 16 scans was used for the FID signal, and, a recycle delay of 2s for the CPMG signal. Bran samples were weighted and placed in climatic chambers at 25 °C under controlled relative humidity of 58% until mass stabilization. Less mobile proton populations, i.e. those having T_2 relaxation times between 0.014 ms and 0.2 ms, were analyzed with the FID measurements, whereas more mobile protons, i.e. those having T_2 relaxation times between 1 ms and 60 ms, were analyzed using the CPMG pulse sequence. The amplitude of proton populations, proportional to their relative quantities is expressed in arbitrary unit and normalized per sample's weight in gram. In the results section, where the proton distributions of the samples are shown, a representative continuous proton distribution of the triplicate measurements was selected. Data were fitted using SigmaPlot and a combination of Sinus cardinal and exponential functions according to the relation:

$$y(t) = A_i e^{-\left(\frac{t}{T_{2i}}\right)^2} \frac{\sin(B * t)}{B * t} + \sum_{i=0}^n A_i e^{-\frac{t}{T_{2i}}} \quad (5)$$

with, A the amplitude; T_2 , the transverse relaxation time; B, a constant; and t, the time.

2.4. Statistical analysis

The statistical significance of results was assessed using Tukey's HSD test. Multiple comparisons were performed by calculating the least significant difference by using the Statgraphics Stratus software. All tests were conducted at 5% significance level.

3. Results & discussion

3.1. Particle size distribution and shape factor

The native brans are both characterized by monomodal distribution of particle diameters but the common wheat bran has significantly higher values of median diameter and span (Fig. 1 and Table 1).

HS circularity values are higher for durum wheat bran (0.36) than for common wheat bran (0.29) but are both lower than the disk reference value equal to 1. This difference highlights more irregular surface and shape for common wheat bran probably related to difference in the mechanical properties.

Grinding operation of brans induced a significant decrease in median diameter and an increase of the span. The particle size of ground durum wheat bran remains always lower than that of common wheat bran, independently of grinder's loading mode. This difference of size among both brans suggests a higher stiffness at ambient conditions, for durum bran in comparison to common bran which leads, for the same amount of milling energy, to smaller particle size.

The particle size distribution of the ground bran is no longer monomodal (Fig. 1) and 2 populations of particles may be observed, with the presence of fine particles with diameters less than 100 μm (Table 1). These fine particles could be attributed to starch granules as it can be seen from their circular shape and size domain around 40 μm (Table 1 and Fig. 1-A1 to B3).

A data analysis was performed to determine the proportion of the 2 populations in ground bran particles and their characteristic criteria (Table 1) by deconvolution of bands into fine or large particles populations. Significant differences in terms of proportions, median diameters and span values are observed. Compared to the impact mill, the centrifugal mill generates, irrespective of the wheat bran type and the mill size grid setting, a higher proportion of fine particles with a small median diameter, and coarse particles with smaller median diameter.

Irrespective of mill grinding mode and wheat bran type, finer milling (grid of 250 or 300 μm) produces a higher proportion of fine particles with a small median diameter and coarse particles with a smaller median diameter.

The span of each population is not significantly impacted by wheat type, mill type and settings. Cadden (1987) reported upon roller grinding of wheat bran that the wheat bran cell wall is disrupted upon grinding and the matrix structure is more prone to collapse affecting thus the porous structure. This effect on the matrix structure was confirmed by SEM (Fig. 1). Ground samples appeared as small fragments of few structures that could be recognized. The shearing forces in centrifugal grinder, applied tangentially to fibers, seem to limit the collapse of the porous structures.

3.2. Composition

The composition of native and ground durum or common wheat brans is reported in Table 2. The two types of brans have initial water contents in the same range. They differ by their starch content more than two time higher in the case of durum wheat.

Both brans also exhibit differences in terms of neutral monosaccharides as reported in Table 2. Durum wheat bran has a slightly

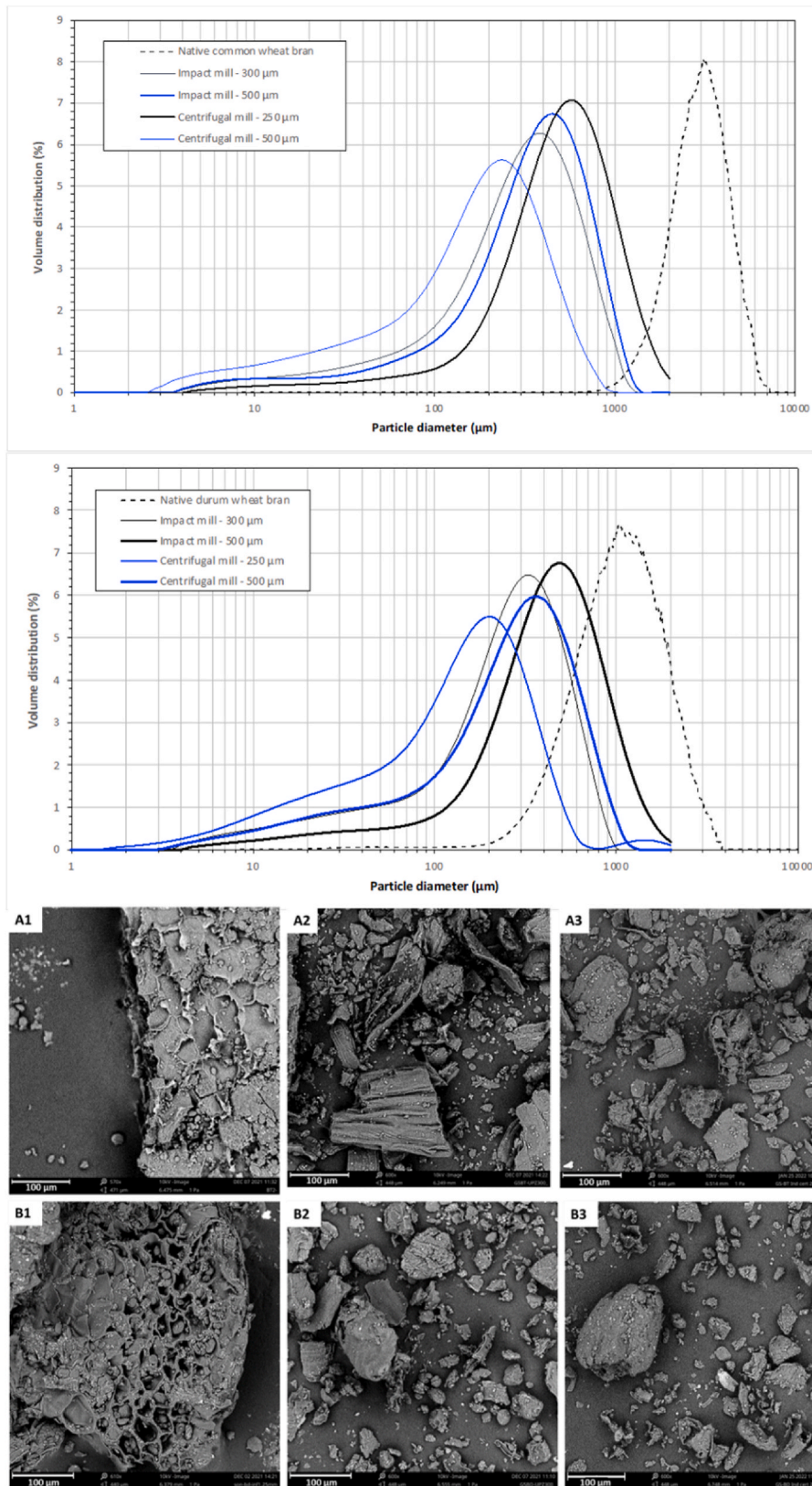


Fig. 1. Particle size distributions for the different native and milled brans from common or durum wheat. SEM observations of native common (A) or durum (B) wheat brans, in native form (A1-B1), ground with impact miller - 300 μm (A2 - B2) or ground with centrifugal grinder - 250 μm (A3-B3).

Table 1

Proportion of fine particles and parameters (median value and span) of distribution curves of particle size for the different milled brans from common or durum wheat. *Circle equivalent diameter indicated as D₅₀ was acquired by granulomorphological analysis for native brans. Cumulated values of 5 plates are represented.

	Proportion of		Finer particles		Larger particles	
	fine particles (%)		D ₅₀ (µm)	Span	D ₅₀ (µm)	Span
<i>Common wheat</i>						
Native bran ^(s)	–		–	–	3225 (± 271)	0.75 (± 0.01)
Impact mill - 300 µm	16.0 (±1.0) ^d		34.4 (±0.4) ^c	2.01 (±0.13) ^{bc}	340 (±11) ^e	1.50 (±0.07) ^{ab}
Impact mill - 500 µm	8.0 (±0.3) ^a		36.0 (±0.4) ^d	2.20 (±0.13) ^e	525 (±6) ^h	1.74 (±0.03) ^c
Centrifugal mill - 250 µm	25.9 (±0.3) ^g		28.2 (±0.2) ^b	1.97 (±0.02) ^{ab}	202 (±1) ^b	1.57 (±0.01) ^b
Centrifugal mill - 500 µm	14.0 (±0.7) ^c		42.9 (±1.8) ^f	1.89 (±0.06) ^a	364 (±13) ^f	1.54 (±0.07) ^{ab}
<i>Durum wheat</i>						
Native bran ^(s)	–		–	–	1125 (± 72)	1.36 (± 0.02)
Impact mill - 300 µm	21.9 (±0.4) ^f		36.0 (±0.6) ^d	2.17 (±0.03) ^{de}	293 (±5) ^c	1.41 (±0.04) ^a
Impact mill - 500 µm	10.3 (±1.1) ^b		36.4 (±0.5) ^d	2.11 (±0.03) ^{cde}	433 (±13) ^g	1.64 (±0.03) ^{bc}
Centrifugal mill - 250 µm	29.0 (±1.8) ^h		24.8 (±0.4) ^a	1.92 (±0.03) ^{ab}	179 (±9) ^a	1.58 (±0.27) ^b
Centrifugal mill - 500 µm	20.1 (±0.4) ^e		37.6 (±0.8) ^e	2.08 (±0.04) ^{cd}	315 (±4) ^d	1.52 (±0.02) ^{ab}

Means in the same column with different letters are significantly different (P < 0.05) by Tukey's HSD test.

Table 2

Composition of common and durum wheat grains and their brans.

	Water (g/100 g dm)	Ash (g/100 g dm)	Total starch (g/100 g dm)	Damaged starch (g/100 g dm)
<i>Common wheat</i>				
Native bran	12.8 ± 0.2	6.24 ± 0.04	8.0 ± 0.4	0.7 ± 0.02
Impact mill - 300 µm	10.1 ± 0.01	6.72 ± 0.02	8.5 ± 0.6	0.9 ± 0.02
Impact mill - 500 µm	10.8 ± 0.1	6.75 ± 0.02	7.1 ± 0.1	0.7 ± 0.01
Centrifugal mill - 250 µm	8.2 ± 0.03	7.07 ± 0.01	8.3 ± 0.05	1.0 ± 0.01
Centrifugal mill - 500 µm	10.2 ± 0.01	7.03 ± 0.03	8.9 ± 0.5	0.9 ± 0.01
<i>Durum wheat</i>				
Native bran	11.5 ± 0.2	5.05 ± 0.04	18.6 ± 0.3	2.0 ± 0.1
Impact mill - 300 µm	10.9 ± 0.03	5.04 ± 0.03	19.4 ± 0.2	2.9 ± 0.1
Impact mill - 500 µm	11.6 ± 0.1	5.04 ± 0.01	21.6 ± 1.0	2.2 ± 0.02
Centrifugal mill - 250 µm	8.7 ± 0.1	4.82 ± 0.07	18.7 ± 0.3	3.5 ± 0.01
Centrifugal mill - 500 µm	10.9 ± 0.1	5.09 ± 0.02	21.6 ± 0.5	2.8 ± 0.1
		Native Common wheat bran		Native Durum wheat bran
Total monosaccharide (g/100 g dm)		51.7 ± 0.41		54.8 ± 1.86
GalA (g/100 g dm)		0.04 ± 0.03		0.54 ± 0.14
GlcA (g/100 g dm)		0.84 ± 0.01		0.76 ± 0.05
Man (g/100 g dm)		0.68 ± 0.04		0.77 ± 0.03
Xyl (g/100 g dm)		16.4 ± 0.11		12.9 ± 0.25
Glc (g/100 g dm)		24.24 ± 0.70		31.47 ± 1.60
Gal (g/100 g dm)		1.10 ± 0.06		1.26 ± 0.08
Rha (g/100 g dm)		0.19 ± 0.05		0.19 ± 0.02
Ara (g/100 g dm)		9.09 ± 0.25		8.22 ± 0.08
Lignin (g/100 g dm)		5.97 ± 0.01		5.28 ± 4.10 ⁻⁴

higher content of neutral monosaccharides than common wheat bran, due to a more important amount of glucose. This is related to its higher content of starch. Cell walls of bran are known to have glucose monomers as a mix of two forms, β-glucan in the aleurone, and cellulose, mostly located in the inner and outer pericarp (Hemery et al., 2007) in proportion of about 3–4 more cellulose than β-glucan. The other major difference is in the xylose and arabinose content with common wheat bran being richer in both constituents suggesting a higher content of arabinoxylan (Beaugrand et al., 2004b). The value of the A/X ratio (arabinose/xylose) reflects the substitution degree and so the relative enzymatic recalcitrance of arabinoxylan (Beaugrand et al., 2004c). The values of 0.63 and 0.55 obtained for durum and common wheat, respectively suggest that the arabinoxylan of durum wheat is more branched. Interestingly, durum bran has also more glucuronic acid (Table 1), known to participate as arabinose do to the branching of the xylan backbone (Beaugrand et al., 2004c), revealing definitively that durum hemicellulose is more branched. In this study, the galacturonic acid (GalA) content generally associated with rhamno-galacturonan I (RGI) pectins is also higher for durum wheat bran, suggesting a higher pectin level. If this amount of GalA can be seen as minor (about 0.5%) in term of the total dry mass, this is significantly enough to have an impact on the functional properties and in this study a significantly higher amount in durum wheat bran is quantified compared to common bran

(about 10 time more).

The strongest difference in composition is observed in the damaged starch content especially for durum wheat bran. A significant increase of 45% and 75% occurs in the case of impact and centrifugal grinders respectively for the lowest grinder grid of 250/300 µm. In comparison, the increasing levels are 28% and 42% in the case of common wheat bran.

Discussion - The structural composition of the durum cell walls seems

Table 3

GAB equation parameters and root-mean-square-error (RMSE) for the common and durum wheat brans treated with several grinding processes.

	M ₀	c	k	A(m ² /g)	RMSE	R ²
<i>Common wheat</i>						
Native bran	7.69	15.19	0.66	269.18	0.12	0.999
Impact mill - 300 µm	7.53	15.37	0.68	263.55	0.11	0.999
Impact mill - 500 µm	7.46	15.32	0.68	261.09	0.10	0.998
Centrifugal mill - 250 µm	7.30	15.53	0.68	255.58	0.13	0.999
Centrifugal mill - 500 µm	7.67	15.41	0.66	268.38	0.10	0.999
<i>Durum wheat</i>						
Native bran	6.97	17.82	0.69	244.08	0.13	0.998
Impact mill - 300 µm	6.88	17.67	0.70	240.66	0.16	0.998
Impact mill - 500 µm	7.52	15.31	0.66	263.25	0.13	0.996
Centrifugal mill - 250 µm	6.54	16.20	0.72	228.75	0.13	0.996
Centrifugal mill - 500 µm	7.12	16.22	0.69	249.23	0.57	0.998

more complex and suggests a reinforced protection structure of physical cell walls. Indeed, the glucuronoarabinoxylan seems more branched (Table 2) which can help crosslinking between polysaccharide chains. Regarding pectins, we can hypothesize that RGI side chains can act as plasticizers in cell walls that undergo large physical remodeling. Regarding the global composition, similar compositions were reported for wheat bran with around 55% of the dietary fibre being arabinoxylan, while the remaining was cellulose (9–12%), lignin (3–5%), fructan (3–4%) and mixed linked β -glucan (2.2–2.6%) (Chalamacharla et al., 2018). The reported ash content was 5.5–6.5%, in line with our values. In the pericarp-seed coat, the higher amount of galactose in common wheat bran suggests the occurrence of complex heteroxylans, previously identified in wheat bran (Brillouet and Joseleau, 1987). Lignin content measured by Klason's method (Table 2) indicates that common wheat bran displays a slightly higher content compared to durum. Lignin distribution has been reported to affect the position of fracture within various cell wall layers (Donaldson, 1995). Increased levels of damaged starch upon grinding are in accordance with previous works on wheat flour, starch damage degree depending on raw materials, particle coarseness and milling conditions (Wang et al., 2020).

3.3. Water vapor adsorption isotherms

Water vapor adsorption isotherm of the two native brans display a classical sigmoidal shaped curve (Fig. A.1).

The GAB model fits well the experimental data ($R^2 > 0.995$) for all samples. The values obtained from the fit are reported in Table 3. The water vapor adsorption ability of common wheat bran water is more pronounced than the lower-sized durum wheat bran and differences are more pronounced in the intermediate "multilayer region" as shown by the higher values of solid surface area, A , for common wheat bran (Table 3).

Solid surface area refers to the total surface area available for hydrophilic binding. It differs from "theoretical surface area" by taking material porosity as well as particle size reduction into account. The calculated values of the GAB model for the monolayer content M_0 for bran were reported to be around 6.6–6.8 g/100 g dm (Li et al., 2021). In our case, these monolayer values were lower for native durum wheat bran indicating lower water adsorption capacities under low relative humidity conditions. The chemical composition is known to influence its water vapor adsorption capacity (Li et al., 2021) and the water holding capacity was positively correlated with the amount of insoluble noncellulosic polysaccharides, and negatively with cellulose and lignin (Dural and Hines, 1993). The transposition to our results must be done with care as the water holding capacity is based on the addition of water in liquid form while water vapor sorption isotherms are based on equilibration in a controlled water vapor atmosphere. With water vapor adsorption isotherms, the direct interactions of wheat bran with the water molecules can be estimated, while with liquid addition only the ability to trap large amounts of water inside macromolecular complexes is taken into account. Our results suggest that the ratio of cellulose-lignin content to hemicellulose content is negatively correlated with its water sorption capacity. The comparative analysis of lignin revealed a comparable amount in common and durum wheat brans. In addition, the higher amount of hemicellulose and pectin in common wheat bran and on another hand the higher amount of glucose-polymer for durum wheat bran are experimental proofs that confirm the coherence of a higher water sorption capacity for common wheat bran.

Grinding tends to decrease the M_0 values as well as the surface area of common wheat brans powders. It tended to increase the value of the k constant in the GAB equation for common wheat bran (Table 3). Similar

trend was reported for ultrafine grinding of wheat bran (Li et al., 2021). This was not that obvious in the case of ground durum wheat bran. The centrifugal shear grinder maintains the same initial differences observed between the two types of bran. The impact grinder with the grid size of 500 μm has the most effect on durum wheat bran reducing the water vapor adsorption differences (fig.A1B) with solid surface area, M_0 , c and k . For all other milling conditions, these values remain in similar range for both types of brans.

Since milling may cause the damage of hydrogen bonding (Wang et al., 2020), the exposition of hydroxyls can be modified upon grinding and may explain the difference observed during impact milling of durum wheat bran.

Discussion - Durum wheat bran appears to be more prone to variations in its sorption behavior as function of mechanical loading mode than common wheat bran, and more pronounced with impact grinders, with an increase of sorption aptitude independently of the grid size highlighted by a higher variation of M_0 and A_0 values (Table 3). Dural and Hines (1993) indicated that the differences in particle size between the ground sample do not allow to explain the variations of the sorption behavior. It can be noted in the SEM images (Fig. 1) that the structure of durum wheat bran seems more porous than that of durum bran. We also pointed out earlier that the bran structure collapsed more with impact milling. This modification of durum wheat bran structure may explain the difference observed in water vapor adsorption behavior.

3.4. ATR-FTIR measurements

ATR-FTIR experiments were conducted on native and ground wheat brans in order to estimate the impact of grinding loading mode on hydration water structuring. The structure and dynamics of bulk water was differentiated from that of hydration water (Bellissent-Funel, 2001), which may result in a three-dimensional transient network in which bonds are constantly breaking and reforming. This approach is not much reported in literature for granular media such as wheat bran.

We focus on the O–H stretching mode $\nu(\text{OH})$ (3700–3000 cm^{-1}) that is especially sensitive to the surrounding hydrogen bond environment and may provide insights on the structure of hydration water (Grossutti et Dutcher, 2016). There exists a variety of water molecules that are differently H bonded to each other, with H-bond coordination numbers ranging from 0 to 4. The low-wavenumber oscillators (centered around 3310 cm^{-1}), called hereafter "network water" (NW), correspond to strongly H-bonded water molecules having a coordination number close to four. The high-wavenumber component (around 3600 cm^{-1}), called "multimer water" (MW), is assigned to water molecules with a small number of H-bonds to other water molecules. In between lies the component centered at 3450 cm^{-1} corresponding to "intermediate water" molecules (labelled IW) (Enev et al., 2019).

Fig. 2A and B shows that the two types of brans differ in the 3700–3100 cm^{-1} region with native common wheat bran having higher absorbance intensity for the 3200 cm^{-1} band, corresponding to strongly bonded water molecules.

Fig. 2A and B shows that multimer water at 3600 cm^{-1} in the case of durum wheat (Fig. 2A) is more disturbed by the grinding loading mode (Fig. 2B). The absorbance of this band decreases mostly with the particle size for the centrifugal shear grinder and we observed a clear redistribution of the 3 water sub-populations. In addition, there is a 17 cm^{-1} shift for the multimer band after all grinding steps implicating a change in interaction energy of hydration water upon grinding. This significant decrease in band's wavenumber is indicative of an increase in the number and strength of hydrogen bonds upon durum wheat bran grinding (Enev et al., 2019). It was reported in literature that this high

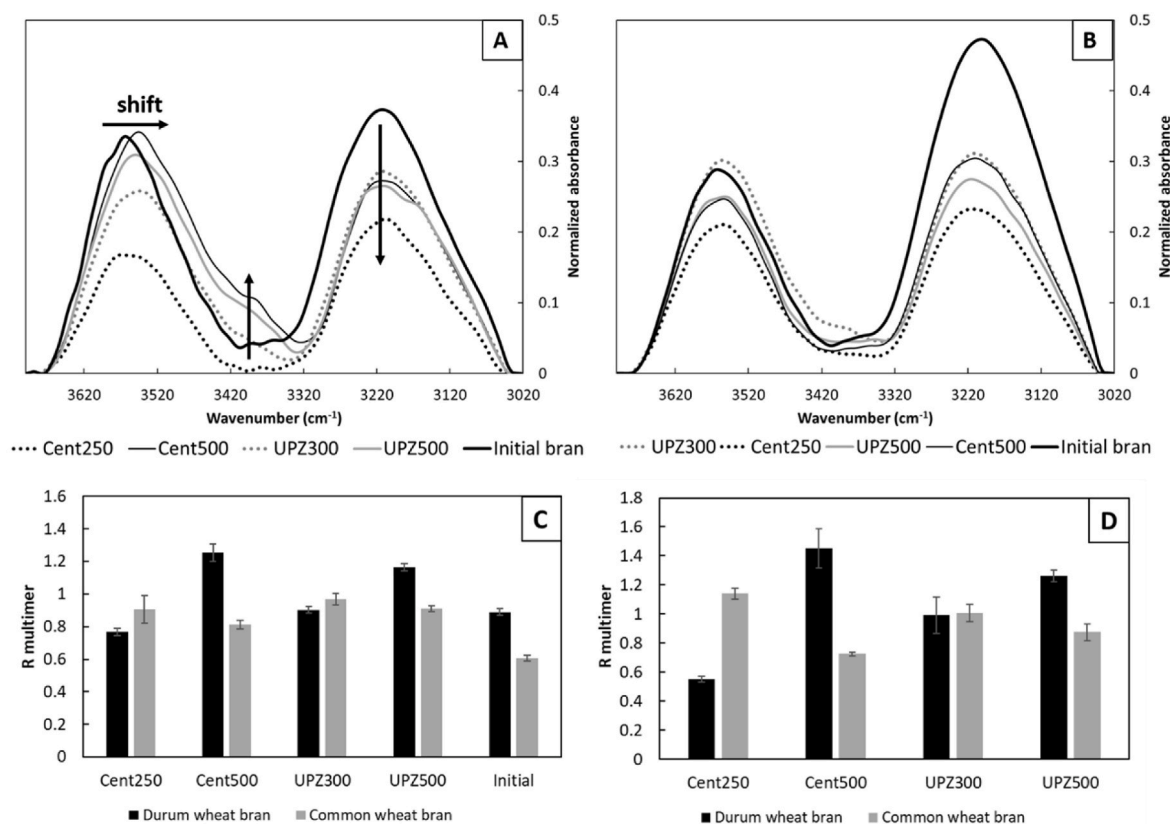


Fig. 2. ATR-FTIR spectra of interface hydration water at different grinding processes of durum (A) and common wheat bran (B) equilibrated at a relative humidity of 58% obtained after subtraction of freeze dried spectra. R_{multimer} calculated for durum wheat and common wheat brans at different grinding processes at a relative humidity of 58% (C) and 40% (D).

frequency band tends to be displaced and less broad in the case of pore size reduction (Le Caër et al., 2011). This is noted in Fig. 2A for the smallest particles (grid sizes of 250 and 300 μm). The gain in the intermediate water zone (at 3400 cm^{-1}) occurs therefore to the detriment of network water (NW) molecules (at 3200 cm^{-1}) for durum wheat bran upon grinding.

In the case of common wheat bran the major difference upon grinding is the reduction of the low wavenumber component's intensity at 3200 cm^{-1} , indicating an increase in the number of network water molecules. The spectral parameter R_{multimer} ($R_{\text{multimer}} = A_{3600}/A_{3200}$) was calculated for each spectrum according to Grossutti and Dutcher (2016). This parameter presented in Fig. 2C and D provides information about the relative population of water molecules in a disrupted hydrogen bond network to those in a well-ordered hydrogen bond network. The spectra were recorded for bran samples equilibrated at 40 or 58% of relative humidity, as to be in the water vapor adsorption isotherms zone where more differences among brans were revealed. R_{multimer} varies more steeply among the 2 types of wheat bran at 40% relative humidity (Fig. 2C and D), indicating the significant impact of early stages of water sorption. Farshchi et al. (2019) demonstrated for spray dried detergent powders that a relative humidity increase induces a higher occupation of polar available sites by water molecules which in turn increases the order of the system and mechanisms of water sorption. At low relative humidity, the mechanism of surface adsorption related to the powder micro-structure may be predominant. However, at medium and high relative humidity values, bulk water sorption mainly predominates.

Discussion - The R_{multimer} is more elevated for durum wheat bran at a larger particle size (500 μm for both impact and centrifugal mills). This is mostly related to the initial differences in raw material properties rather than size reduction or loading mode. The difference in the evolution of the R_{multimer} between the 2 types of bran suggests potential changes in physicochemical and hydration properties upon milling. The functional groups and/or their accessibility can be altered by the grinding loading mode impacting the network water component situated at low wavenumbers. Regarding damaged starch, durum wheat bran had the highest values initially and after all grinding processing (Table 2). Durum wheat bran ground with impact grinder expressed the greater reduction of the 1030:997 cm^{-1} ratio band (a reduction of about 17% at both grid sizes vs 1.5% for common wheat bran) and an additional red shift of 8–12 cm^{-1} in the band at 1030 cm^{-1} upon grinding (vs no shift for common wheat bran). This is in line with water vapor adsorption isotherms trends for durum wheat bran. Roa et al. (2014) also demonstrated that ball-milling treatment of amaranth grain significantly decreased the intensity ratios of the band 1039 and 1014 cm^{-1} corresponding to the crystalline/amorphous part of starch structure.

The centrifugal shear miller increases the FTIR signal associated with the relative content of the water strongly bound in the hydration layer of bran. This effect seems more pronounced for the durum wheat bran with the centrifugal miller and a grid of 500 μm . Rupturing of the cell walls in bran through the actions of impact forces and friction upon milling might result in cleavage of covalent bonds (Jacobs et al., 2015). The same forces can be held responsible for the increase in damaged starch

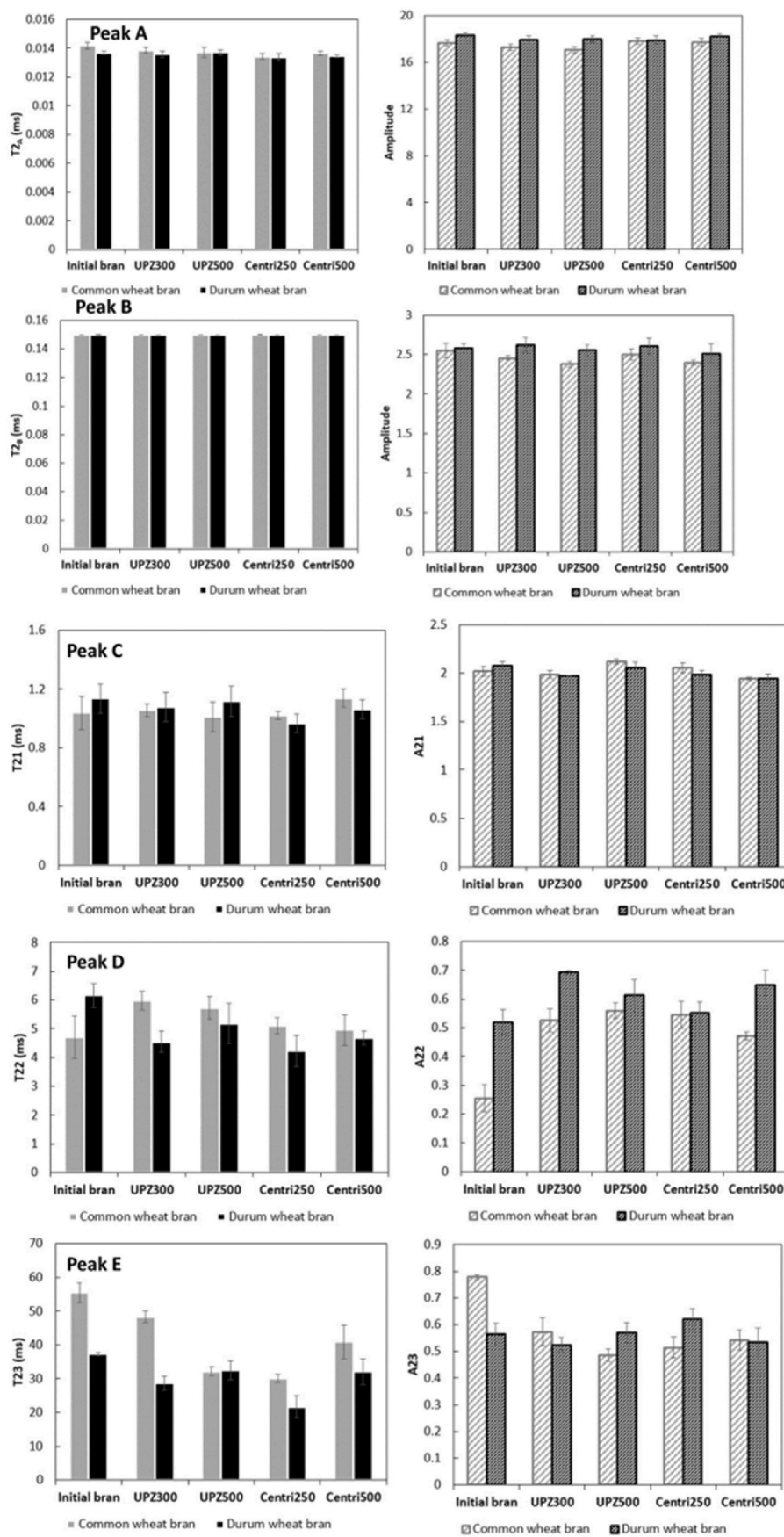


Fig. 3. FID and Carr-Purcell-Meiboom-Gill (CPMG) proton distributions of common and durum wheat brans at different grinding conditions. Free induction decay proton distributions of wheat brans with relaxation time T2 and amplitude.

with this centrifugal shear grinder (Table 2).

3.5. Low field NMR measurements

Different states of water binding (little, medium, or very mobile water) can be distinguished using low field NMR methods. The use of Carr–Purcell–Meiboom–Gill (CPMG) sequences allows the determination of the transverse relaxation time (T2) that describes the interactions between water and components, their intensity and the amount of water involved. Systems with low proton mobility have short T2 of the order of a few μ s. Systems with high proton mobility have shorter interaction times to exchange energy, and therefore longer T2 of the order of 1 s.

NMR results (Fig. 3) show two FID populations around 0.014 and 0.15 ms (peaks A and B) and three CPMG populations at 1, 4–6 ms and 30–60 ms (peaks C, D, and E). Based on the work on wheat bran of Hemdane et al. (2017), population A could be attributed to protons of densely packed arabinoxylan and probably also to those of crystalline cellulose. Populations B and C are less straight-forward to define, but could comprise most likely CH-protons of arabinoxylan, given their comparable distribution with arabinoxylan and their low mobility. Population D can be assigned to OH protons of water interacting with bran-related biopolymers such as arabinoxylan and cellulose as well as protons of intragranular water. Population E representing the most mobile proton population can only be assigned to water held through improper stacking, and not by intragranular water.

The major differences between the two brans ground in the different milling conditions are in the high mobility water (observed in peak E). Relaxation time T2 of peak E (Fig. 3) is significantly lower for the initial and ground durum wheat bran (all processing conditions), the lowest value being obtained with the centrifugal shear grinder with a 250 μ m grid.

In addition, T2 relaxation times are always lower for native and ground durum wheat bran for the high mobility water peak (peak E). Less mobile water is thus present for durum wheat bran. This is in line with higher $R_{multimer}$ as seen in ATR-FTIR measurements, indicative of more interactions between bran matrix and water.

Discussion - Similar results of differences in high mobility water were observed by Hemdane et al. (2017) on coarse and ground wheat brans. They suggest less interactions between water molecules and the bran's backbone related to the mechanical loading mode constraints which create disturbances. These observations are in accordance with those from the water vapor adsorption isotherms of durum wheat bran for values in the region 0.4–0.8 corresponding to the intermediate and most mobile water. For the comparison of bran between them, the main differences are evidenced at the lowest particle sizes of 250 μ m and 300 μ m

in centrifugal grinders and impact grinders respectively.

The mechanisms responsible of the interaction between water and bran components are not yet fully elucidated. In wheat bran, Jacobs et al. (2015) suggested that strongly bound water may be related to capillary action (nano-pores) and strong hydrogen bonds, whereas weakly bound water mainly arises from the filling of micropores and stacking phenomena.

4. Conclusion

The present study investigates the effect of grinding loading modes on intrinsic hydration properties as function of type of bran (common vs durum wheat bran). The results from water vapor adsorption isotherms, FTIR and NMR experiments suggested that grinding is not limited to size reduction and also affect the physical structure of the bran particles and generated modifications of bran structure that can be evidenced by the strength of the bran-water interactions. These effects are depending on the type of bran, and on the type of main loading mode generated by the milling device and their mechanical work intensities. Native durum wheat bran has lower water vapor adsorption capacities than common wheat bran due to differences in chemical composition and particle characteristics. The water vapor adsorption capacities of durum wheat bran are more affected by the milling process.

During the milling process of common wheat bran, shear with a middle intensity mechanical work (size grid of 500 μ m) tends to increase the proportion of strongly bound water, probably related to the opening of cell wall. By contrast impact milling tends to reduce the water vapor adsorption capacity by collapsing the porous structure of the wheat bran particles. For durum wheat bran, the effect for shear milling with high mechanical work (size grid of 300 μ m) and for impact milling are in between these two behaviors as they probably result of a competition between the opening of new cell wall during the grinding and the collapsing of the structure durum wheat structure. Complementary studies are needed to clarify the relation between the effect of the grinding mode on the dissociation of the tissues and on the accessibility of the constituents and their impact on the hydration properties. This will bring new elements to optimize the milling processability of wheat bran to target specific hydration properties to cereals products enriched in bran.

Funding source

This work was supported by BPI France through the research program “DEFI Blé Dur”.

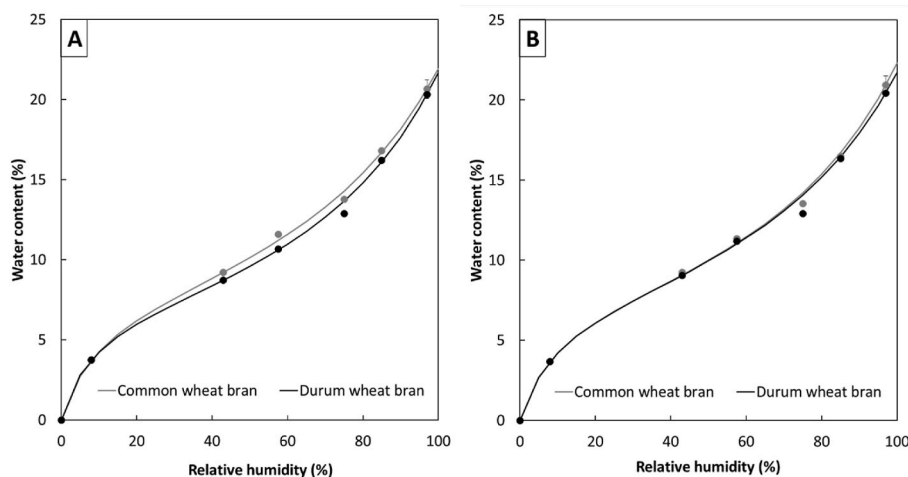


Fig. A.1. Water vapor adsorption isotherms of native brans from durum wheat and common wheat (A) and of ground brans after UPZ grinder and 500 μ m grid (B). Circle dots are experimental values and line is calculated curves with the GAB model. Mean values of duplicate measurements are represented.

Author statement

Reine Barbar: Conceptualization, investigation, formal analysis, Writing-original draft, project administration. Claire Mayer-Laigle: Conceptualization, writing-reviewing and editing, supervision. Johnny Beaugrand: Investigation, writing-reviewing and editing. Bernard Cuq: Formal analysis, funding acquisition, writing-reviewing and editing. Cécile Barron: Supervision, methodology, writing-reviewing and editing.

Declaration of competing interest

The authors declare that they have no known competing financial interests or personal relationships that could have appeared to influence the work reported in this paper.

Data availability

Data will be made available on request.

Acknowledgment

The authors thank the PLANET facility (<https://doi.org/10.15454/1.5572338990609338E12>) run by the IATE joint research unit for providing process experimental support. We acknowledge the support of Dr. Veronica MEJIA TAMAYO in NMR experiments and data analysis. Johnny Beaugrand thanks both Méline Calatraba (BIA, Nantes) for her skills in biochemical analysis and Nathalie Boizot (Phenobois, Orléans) for the Klason lignin quantification.

References

- Barteau, G., Azoti, W., Gautreau, M., Francart, C., Alès, G., Jmal, H., Bouchet, J., Kervoelen, A., Beaugrand, J., Bahlouli, N., Bourmaud, A., 2021. Recycling of wood-reinforced poly-(propylene) composites: a numerical and experimental approach. *Ind. Crops Prod.* 167, 113518 <https://doi.org/10.1016/j.indcrop.2021.113518>.
- Beaugrand, J., Cronier, D., Thiebeau, P., Schreiber, L., Debeire, P., Chabbert, B., 2004a. Structure, chemical composition, and xylanase degradation of external layers isolated from developing wheat grain. *J. Agric. Food Chem.* 52, 7108–7117. <https://doi.org/10.1021/jf049529w>.
- Beaugrand, J., Reis, D., Guillon, F., Debeire, P., Chabbert, B., 2004b. Xylanase-mediated hydrolysis of wheat bran: evidence for subcellular heterogeneity of cell walls. *Int. J. Plant Sci.* 165, 553–563. <https://doi.org/10.1086/386554>.
- Beaugrand, J., Chambat, G., Wong, V.W.K., Goubet, F., Rémond, C., Paës, G., Benamrouche, S., Debeire, P., O'Donohue, M., Chabbert, B., 2004c. Impact and efficiency of GH10 and GH11 thermostable endoxylanases on wheat bran and alkali-extractable arabinoxylans. *Carbohydr. Res.* 339, 2529–2540. <https://doi.org/10.1016/j.carres.2004.08.012>.
- Bellissent-Funel, M.-C., 2001. Structure of confined water. *J. Condens. Matter Phys.* 13, 9165–9177. <https://doi.org/10.1088/0953-8984/13/41/308>.
- Blumenkr, N., Asbohan, G., 1973. New method for quantitative determination of uronic acids. *Anal. Biochem.* 54, 484–489. [https://doi.org/10.1016/0003-2697\(73\)90377-1](https://doi.org/10.1016/0003-2697(73)90377-1).
- Brillouet, J.M., Joseleau, J.P., 1987. Investigation of the structure of a heteroxylan from the outer pericarp (beeswing bran) of wheat bran. *Carbohydr. Res.* 159, 109–126. [https://doi.org/10.1016/S0008-6215\(00\)90009-0](https://doi.org/10.1016/S0008-6215(00)90009-0).
- Cadden, A.-M., 1987. Comparative effects of particle size reduction on physical structure and water binding properties of several plant fibers. *J. Food Sci.* 52, 1595–1599. <https://doi.org/10.1111/j.1365-2621.1987.tb05886.x>.
- Chalamacharla, R.B., Harsha, K., Sheik, K.B., Viswanatha, C.K., 2018. Wheat bran-composition and nutritional quality: a review. *Adv. Biotech. & Micro.* 9, 555754 <https://doi.org/10.19080/AIBM.2018.09.555754>.
- Ciccoritti, R., Taddei, F., Nicoletti, I., Gazza, L., Corradini, D., D'Egidio, M.G., Martini, D., 2017. Use of bran fractions and debranned kernels for the development of pasta with high nutritional and healthy potential. *Food Chem.* 225, 77–86. <https://doi.org/10.1016/j.foodchem.2017.01.005>.
- Deroover, L., Tie, Y., Verspreet, J., Courtin, C.M., Verbeke, K., 2020. Modifying wheat bran to improve its health benefits. *Crit. Rev. Food Sci. Nutr.* 60, 1104–1122. <https://doi.org/10.1080/10408398.2018.1558394>.
- Donaldson, L.A., 1995. Cell wall fracture properties in relation to lignin distribution and cell dimensions among three genetic groups of radiata pine. *Wood Sci. Technol.* 29, 51–63. <https://doi.org/10.1007/BF00196931>.
- Dural, N.H., Hines, A.L., 1993. Adsorption of water on cereal-bread type dietary fibers. *J. Food Eng.* 20, 17–43. [https://doi.org/10.1016/0260-8774\(93\)90017-E](https://doi.org/10.1016/0260-8774(93)90017-E).
- Enev, V., Sedláček, P., Jarábková, S., Velcer, T., Pekař, M., 2019. ATR-FTIR spectroscopy and thermogravimetry characterization of water in polyelectrolyte-surfactant hydrogels. *Colloids Surf. A Physicochem. Eng. Asp.* 575 (2019), 1–9. <https://doi.org/10.1016/j.colsurfa.2019.04.089>.
- Farshchi, A., Hassanpour, A., Bayly, A.E., 2019. The structure of spray-dried detergent powders. *Powder Technol.* 355, 738–754. <https://doi.org/10.1016/j.powtec.2019.06.049>.
- Grossutti, M., Dutcher, J.R., 2016. Correlation between chain architecture and hydration water. *Biomacromolecules* 17, 1198–1204. <https://doi.org/10.1021/acs.biomac.6b00026>.
- Hemdane, S., Jacobs, P.G., Bosmans, G.M., Verspreet, J., Delcour, J.A., Courtin, C.M., 2017. Study of biopolymer mobility and water dynamics in wheat bran using time-domain 1H NMR relaxometry. *Food Chem.* 236, 68–75. <https://doi.org/10.1016/j.foodchem.2017.01.020>.
- Hemery, Y., Rouau, X., Lullien-Pellerin, V., Barron, C., Abecassis, J., 2007. Dry processes to develop wheat fractions and products with enhanced nutritional quality. *J. Cereal. Sci.* 46, 327–347. <https://doi.org/10.1016/j.jcs.2007.09.008>.
- Jacobs, P.J., Hemdane, S., Dornez, E., Delcour, J.A., Courtin, C.M., 2015. Study of hydration properties of wheat bran as a function of particle size. *Food Chem.* 179, 296–304. <https://doi.org/10.1016/j.foodchem.2015.01.117>.
- Le Caër, S., Pin, S., Esnouf, S., Raffy, Q., Renault, J. Ph, Brubach, J.-B., Creff, G., Roy, P., 2011. A trapped water network in nanoporous material: the role of interfaces. *Phys. Chem. Chem. Phys.* 13, 17658–17666. <https://doi.org/10.1039/C1CP21980D>.
- Li, X., Han, X., Tao, L., Jiang, P., Qin, W., 2021. Sorption equilibrium moisture and isosteric heat of Chinese wheat bran products added to rice to increase its dietary fibre content. *Grain Oil Sci. Technol.* 4, 149–164. <https://doi.org/10.1016/j.gaost.2021.09.001>.
- Mayer-Laigle, C., Barakat, A., Barron, C., Delenue, J.Y., Frank, X., Mabilie, F., Rouau, X., Sadoudi, A., Samson, M.-F., Lullien-Pellerin, V., 2018. Dry biorefineries: multiscale modeling studies and innovative processing. *Innovat. Food Sci. Emerg. Technol.* 46, 131–139. <https://doi.org/10.1016/j.ifset.2017.08.006>.
- Mazza, G., Le Maguer, M., 1978. Water sorption properties of yellow globe onion (*Allium cepa* L.). *Can. Inst. Food Sci. Technol. J.* 11, 189. [https://doi.org/10.1016/S0315-5463\(78\)73269-4](https://doi.org/10.1016/S0315-5463(78)73269-4).
- Monties, B., 1984. Determination of acid-insoluble lignin – effect of pretreatment acid-hydrolysis on the Klason lignin in wood and straw. *Agronomie* 4, 387–392.
- Onipe, O.O., Jideani, A.I.O., Beswa, D., 2015. Composition and functionality of wheat bran and its application in some cereal food products. *Int. J. Food Sci. Technol.* 50, 2509–2518. <https://doi.org/10.1111/ijfs.12935>.
- Poole, P.L., Finney, J.L., 1982. A direct difference infrared cell for studying the hydration of protein glasses. *J. Phys. E Sci. Instrum.* 15, 1073–1076. <https://doi.org/10.1088/0022-3735/15/10/028>.
- Roa, D.F., Santagapita, P.R., Buera, M.P., Tolaba, M.P., 2014. Ball milling of amaranth starch-enriched fraction. changes on particle size, starch crystallinity, and functionality as a function of milling energy. *Food Bioprocess Technol.* 7, 2723–2731. <https://doi.org/10.1007/s11947-014-1283-0>.
- Stevenson, L., Phillips, F., O'Sullivan, K., Walton, J., 2012. Wheat bran: its composition and benefits to health, a European perspective. *Int. J. Food Sci. Nutr.* 63, 1001–1013. <https://doi.org/10.3109/09637486.2012.687366>.
- Wang, Q., Li, L., Zheng, X., 2020. A review of milling damaged starch: generation, measurement, functionality and its effect on starch-based food systems. *Food Chem.* 315, 126267 <https://doi.org/10.1016/j.foodchem.2020.126267>.
- Wu, H., Flint, A.J., Qi, Q., van Dam, R.M., Sampson, L.A., Rimm, E.B., Holmes, M.D., Willett, W.C., Hu, F.B., Sun, Q., 2015. Association between dietary whole grain intake and risk of mortality: two large prospective studies in US men and women. *JAMA Intern. Med.* 175, 373–384. <https://doi.org/10.1001/jamainternmed.2014.6283>.